Universal fine structure of nematic hedgehogs

2001 J. Phys. A: Math. Gen. 34 829

(http://iopscience.iop.org/0305-4470/34/4/309)

INSTITUTE OF PHYSICS PUBLISHING JOURNAL OF PHYSICS A: MATHEMATICAL AND GENERAL

J. Phys. A: Math. Gen. **34** (2001) 829–838 www.iop.org/Journals/ja PII: S0305-4470(01)15759-8

Universal fine structure of nematic hedgehogs

Samo Kralj[1] **and Epifanio G Virga**[2]

[1] Laboratory Physics of Complex Systems, Faculty of Education, University of Maribor, Koroška 160, 2000 Maribor, Slovenia
and
Solid State Group, Institute Jožef Stefan, Jamova 39, 1000 Ljubljana, Slovenia
[2] Department of Mathematics, INFM Research Unit, University of Pavia, via Ferrata 1, 27100 Pavia, Italy

Received 18 July 2000, in final form 9 November 2000

Abstract

We study in a Landau–de Gennes approach the biaxial structure of a nematic point defect with topological charge $M = +1$. We aim to illuminate the role of the confining boundaries in determining the fine structure of the defect. We show that there are different regimes associated with different values of the ratio between the typical size R of the region in space occupied by the material and the biaxial correlation length ξ_b. For $R/\xi_b > 20$ the core structure is already qualitatively universal, that is, independent of the confining geometry, while also for $R/\xi_b > 200$ any quantitative difference is unlikely to be detected.

PACS numbers: 6130, 6130J, 6172B

1. Introduction

Defects play an important role in a number of areas in physics [1]. In different media they are also referred to as disclinations, dislocations, vortices or strings. Topological defects in ordered media correspond to regions where a configuration of the relevant order parameter field cannot be transformed into a ground state via continuous deformations without affecting the far field [1]. The net advantage in studying defects is that they exhibit many universal features [1–3], so that a single special system can serve as a paradigm in the study of many phenomena. Various liquid crystal phases are especially fit for this purpose because they can easily be accessed experimentally and they exhibit almost all kinds of defects [2, 4].

The simplest liquid crystals are nematic; they consist of elongated molecules characterized by a long-range orientational ordering (see, e.g., chapter 2 of [5]). A local average molecular orientation is conventionally described by the uniaxial director $\boldsymbol{n}$, with both $\boldsymbol{n}$ and $-\boldsymbol{n}$ corresponding to the same physical state (this is also called the head–tail invariance). In the bulk ground state $\boldsymbol{n}$ is homogeneously aligned along a generic symmetry-breaking direction. Defects in nematic liquid crystals are classified in terms of the topological charge M, which depends on the director field surrounding the defect [1]. Either point or line defects exist, characterized by an integer or half-integer M. In most cases the free energy associated with

0305-4470/01/040829+10$30.00

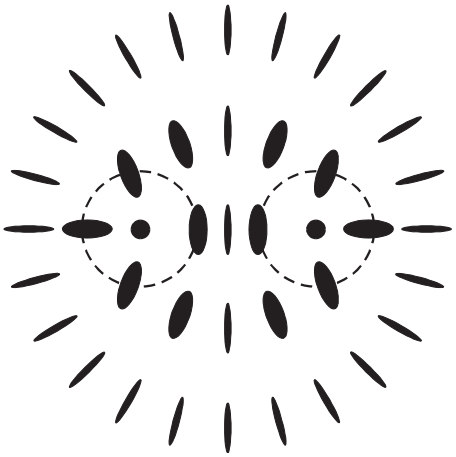

Figure 1. Schematic representation of the biaxial core of a hedgehog. We show the section with a plane through the symmetry axis of the core. The ellipses suggest the molecular orientation on this section: the points where they degenerate in a disc are traversed by the uniaxial ring with negative scalar order parameter, which comes out of the page; accordingly, the broken circles show the trace of the torus with a maximum degree of biaxiality. Both the symmetry axis and the far director field are uniaxial with positive scalar order parameter.

a defect is proportional to M^2, so that defects with low topological charges are preferred: precisely, $M = \pm 1$ for point defects and $M = \pm\frac{1}{2}$ for line defects.

The point defects with $M = +1$ are referred to as *hedgehogs*. They are often pictured as point-like objects with an inner structure. Generally, a director field fails to describe their *core*: sometimes, an extra scalar order parameter suffices. This is the *uniaxial* hedgehog, where the centre of the core is isotropic and surrounded by a spherically symmetric uniaxial paranematic ordering [6–9]. The core size is roughly given by the nematic uniaxial correlation length ξ_n.

More often, the core exhibits a cylindrically symmetric structure characterized by a uniaxial ring [9, 11–14] embedded in a torus with maximal degree of biaxiality [15][3]. This structure is strongly biaxial and requires at least a tensorial description of the local nematic ordering. A symmetric traceless tensor $\boldsymbol{Q}$ proves useful in representing all admissible states (cf p 56 of [5] and section 2 below). The essential features of the distribution in space of the molecular orientational order is depicted schematically in figure 1, where a field of ellipses describes both eigenvalues and eigenvectors of the tensor $\boldsymbol{Q} + \frac{1}{3}\boldsymbol{I}$ on every longitudinal section of the defect core[4]. The long axis of the ellipses represents the preferred molecular orientation on this section; accordingly, a circle represents an isotropic planar molecular distribution. In this picture, the uniaxial ring crosses the longitudinal section precisely at the two points where the ellipses degenerate into a circle. In more technical language (see, for example, [8, 12]), we say that the states along the ring are uniaxial with a negative scalar order parameter and nematic director everywhere tangent to the ring, meaning that the nematic molecules tend to be spread orthogonally to the director. Contrariwise, the states along the symmetry axis of this structure are uniaxial with a positive scalar order parameter and nematic director everywhere parallel to the axis. Figure 1 also illustrates the cross section of the torus with maximal biaxiality found in [15]: here the ellipses representing the local orientational order become distorted the most. The characteristic sizes of both ring and torus are determined by the nematic biaxial correlation length ξ_b defined below. Away from the torus, where a positive uniaxial ordering is soon recovered, the director field is essentially radial relative to the core, though in part presumably affected by the far director field imposed by the boundary conditions.

[3] Another, more complex core structure, referred to as a *core split*, was analysed recently in [10]; however, this is never absolutely stable, though it could be metastable for appropriate temperatures and within a restricted class of competing structures.

[4] Here $\boldsymbol{I}$ denotes the identity tensor.

Despite the fact that the fine equilibrium structure of point defects is rather well explored, several problems still remain open: in particular, the confining effect of the boundary conditions, the role of the core in the interaction between defects and in their non-equilibrium dynamics. Here we focus our attention on the influence of both the confining geometry and its typical size R on the biaxial structure of a point defect with $M = +1$. This paper mainly concerns the spherical confinement, as the cylindrical case has already been examined in detail in [15]. By comparing the results of our analysis in the two cases we conclude that the core structure of a hedgehog becomes universal for R large enough, when it ceases to be affected by the far director field.

The plan of the paper is as follows. In section 2 we outline the mathematical model employed here. In section 3 we compare the effect on the defect core of both cylindrical and spherical confinements. In section 4, we explore the stability of the ring structure against the uniaxial hedgehog. Finally, in the last section we summarize the main conclusion of the paper.

2. Mathematical model

In this section we recall the mathematical model introduced in [15] to describe the fine structure of a hedgehog in a capillary tube and we adapt it to a hedgehog within a spherical cavity.

2.1. Landau–de Gennes approach

We describe nematic states through an order tensor $\boldsymbol{Q}$, which is both symmetric and traceless. In its eigenframe it can be expressed as

$$\boldsymbol{Q} = \sum_{i=1}^{3} q_i \boldsymbol{e}_i \otimes \boldsymbol{e}_i \tag{1}$$

where $\boldsymbol{e}_i$, for $i = 1, 2, 3$, are the eigenvectors and q_i the corresponding eigenvalues [8, 16]. In the uniaxial limit, $\boldsymbol{Q}$ reduces to

$$\boldsymbol{Q} = s\left(\boldsymbol{n} \otimes \boldsymbol{n} - \tfrac{1}{3}\boldsymbol{I}\right) \tag{2}$$

where $\boldsymbol{n}$ is the nematic director and s the scalar uniaxial order parameter. According to [17] the degree of biaxiality is defined as

$$\beta^2 := 1 - 6\,\frac{(\operatorname{tr}\boldsymbol{Q}^3)^2}{(\operatorname{tr}\boldsymbol{Q}^2)^3} \tag{3}$$

and ranges in the interval [0, 1]. In all uniaxial states $\beta^2 = 0$, while states with maximal biaxiality correspond to $\beta^2 = 1$.

In this tensorial representation of nematics the Landau–de Gennes free energy F is expressed as

$$F = \int (A(T - T_*)\operatorname{tr}\boldsymbol{Q}^2 - B\operatorname{tr}\boldsymbol{Q}^3 + C(\operatorname{tr}\boldsymbol{Q}^2)^2 + L|\nabla\boldsymbol{Q}|^2)\,\mathrm{d}v \tag{4}$$

where v is the volume measure, A, B and C are positive material constants, T is the temperature and T_* is the nematic *supercooling* temperature. The elastic properties of the system are described by a single elastic constant L which is independent of the temperature (see also [18]).

We further adopt Lyuksyutov's constraint [19], which reads as

$$\operatorname{tr}\boldsymbol{Q}^2 = \frac{A(T_* - T)}{2C}. \tag{5}$$

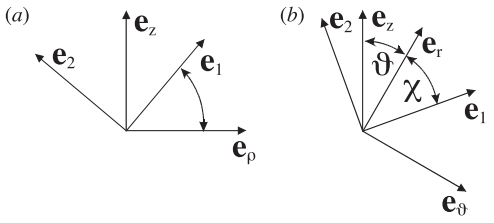

Figure 2. Parametrization for the eigenframe of $\boldsymbol{Q}$ both in (*a*) cylindrical and (*b*) spherical coordinates.

Thus we assume that in nematics local distortions are only produced by reorientations of the eigenvectors $\boldsymbol{e}_i$ or exchanges in the eigenvalues q_i. Within this approximation all distortions that would require melting of the nematic order, attained at $\boldsymbol{Q} = \boldsymbol{0}$, are avoided by entering biaxial states. This is a reasonable assumption as long as the material constant B is considerably smaller than both A and C, as is the case in a typical nematic phase (other applications of this constraint can be found in [8, 12, 15]).

2.2. Parametrization

Since here we study the effect of both cylindrical and spherical confinements on the core of a point defect, we need to resort to both cylindrical and spherical coordinates, which are denoted by $\{\rho, \varphi, z\}$ and $\{r, \vartheta, \varphi\}$, respectively: the corresponding unit vectors along the coordinate axes are $\{\boldsymbol{e}_\rho, \boldsymbol{e}_\varphi, \boldsymbol{e}_z\}$ and $\{\boldsymbol{e}_r, \boldsymbol{e}_\vartheta, \boldsymbol{e}_\varphi\}$. The defect is set at $(\rho, z) = (0, 0)$ in the former coordinate system and at $r = 0$ in the latter: the symmetry axis is $\boldsymbol{e}_z$ in both cases, though it is represented as either $\rho = 0$ or $\vartheta = 0$. We confine attention to nematic distortions described by tensors $\boldsymbol{Q}$ with an eigenvector along $\boldsymbol{e}_\varphi$ in both symmetries. By Lyuksyutov's constraint (5), all such tensors can be represented through the following parametrization [8, 15] (see figure 2):

$$\begin{aligned} \boldsymbol{e}_1^{(\mathrm{c})} &= \cos\kappa\, \boldsymbol{e}_\rho + \sin\kappa\, \boldsymbol{e}_z & \boldsymbol{e}_1^{(\mathrm{s})} &= \cos\chi\, \boldsymbol{e}_r + \sin\chi\, \boldsymbol{e}_\vartheta \\ \boldsymbol{e}_2^{(\mathrm{c})} &= -\sin\kappa\, \boldsymbol{e}_\rho + \cos\kappa\, \boldsymbol{e}_z & \boldsymbol{e}_2^{(\mathrm{s})} &= \sin\chi\, \boldsymbol{e}_r - \cos\chi\, \boldsymbol{e}_\vartheta \\ \boldsymbol{e}_3 &= \boldsymbol{e}_\varphi \end{aligned} \tag{6}$$

and

$$\begin{aligned} q_1 &= \tfrac{2}{3} s_{\mathrm{eq}} \cos\psi & q_2 &= -\tfrac{2}{3} s_{\mathrm{eq}} \cos\left(\psi + \tfrac{1}{3}\pi\right) \\ q_3 &= -\tfrac{2}{3} s_{\mathrm{eq}} \cos\left(\psi - \tfrac{1}{3}\pi\right). \end{aligned} \tag{7}$$

Henceforth the superscripts (c) and (s) denote cylindrical and spherical confinement, respectively. In equation (7) s_{eq} is the equilibrium value of the uniaxial scalar order parameter: it is a function of the temperature such that (5) can also be written as

$$\operatorname{tr} \boldsymbol{Q}^2 = \tfrac{2}{3} s_{\mathrm{eq}}^2.$$

The angle ψ, which ranges over $[-\pi, \pi]$, describes the eigenvalues of $\boldsymbol{Q}$. As explained in detail in [8, 15], it represents both uniaxial and biaxial states. The angles κ and χ determine the orientation of the eigenvectors of $\boldsymbol{Q}$ relative to the axes of the corresponding coordinate system (figure 2). It is indeed a merit of Lyuksyutov's constraint if only two scalars suffice to describe all admissible tensors $\boldsymbol{Q}$. We further simplify the problem by taking $\boldsymbol{Q}$ as a function of (ρ, z) or (r, ϑ) in the cylindrical or spherical confinement. In both cases, we do not consider twisted distortions that would make $\boldsymbol{Q}$ depend on φ.

As remarked in [15], this parametrization fails to be injective: there are transformations in the parameter spaces that leave $\boldsymbol{Q}$ unchanged. The one that plays an important role in our development is

$$\boldsymbol{Q}(\alpha, \psi) = \boldsymbol{Q}(\alpha \pm \tfrac{1}{2}\pi, \tfrac{2}{3}\pi - \psi) \tag{8}$$

where α is either κ or χ. It ensures that both α and ψ can suffer a jump without any discontinuity in $\boldsymbol{Q}$. We refer the reader to [12, 15] for more details on how this ambiguity is exploited to describe the uniaxial ring in the biaxial structure of a point defect.

2.3. Dimensionless free energy

When strong anchoring conditions are imposed on the confining boundary, be it a cylinder or a sphere, the only characteristic lengths entering the model are the biaxial correlation length $\xi_b := \sqrt{\frac{2L}{3Bs_{\rm eq}}}$ and the radius R of either confining cavity. We measure all lengths relative to R so that $\rho \to R\rho$, $z \to Rz$, $r \to Rr$, $\xi_b \to R\xi_b$, $\nabla \to \frac{1}{R}\nabla$; in these units $R = 1$. We measure the free energy F in terms of $F_0 := RLs_{\rm eq}^2$: thus, in the following $F \to F_0 F$. For convenience, we also define the *excess* free energy as $\Delta F := F - F_{\rm bulk}$, where $F_{\rm bulk}$ denotes the free energy of a nematic undistorted in the bulk.

For the two different confinements considered here, ΔF is delivered by the integrals

$$\begin{aligned}\Delta F^{(\rm c)} &= 2\pi \int_{-h/2}^{+h/2} {\rm d}z \int_0^1 {\rm d}\rho\, \rho \Delta f^{(\rm c)} \\ \Delta F^{(\rm s)} &= 2\pi \int_0^1 {\rm d}r\, r^2 \int_0^\pi {\rm d}\vartheta\, \sin\vartheta\, \Delta f^{(\rm s)}\end{aligned} \tag{9}$$

where h is the dimensionless height of the cylinder, and both excess free energies densities have the structure

$$\Delta f = \frac{1}{\xi_b^2}\sigma_b + \sigma_e.$$

The bulk potential term σ_b is the same for both confinements:

$$\sigma_b = \tfrac{4}{27}(1 - \cos 3\psi) \tag{10}$$

while the elastic term σ_e is given by the following expressions:

$$\begin{aligned}\sigma_e^{(\rm c)} = \frac{8}{3}\Bigg[&\frac{1}{4}\left(\left(\frac{\partial\psi}{\partial\rho}\right)^2 + \left(\frac{\partial\psi}{\partial z}\right)^2\right) + \sin^2\left(\psi - \frac{\pi}{3}\right)\left(\left(\frac{\partial\kappa}{\partial\rho}\right)^2 + \left(\frac{\partial\kappa}{\partial z}\right)^2\right) \\ &+ \frac{1}{\rho^2}\left(\sin^2\left(\psi + \frac{\pi}{3}\right)\cos^2\kappa + \sin^2\psi\sin^2\kappa\right)\Bigg]\end{aligned} \tag{11}$$

$$\begin{aligned}\sigma_e^{(\rm s)} = &\frac{2}{3}\left(\left(\frac{\partial\psi}{\partial r}\right)^2 + \frac{1}{r^2}\left(\frac{\partial\psi}{\partial\vartheta}\right)^2\right) \\ &+ \frac{8}{9}\left(\cos\psi + \cos\left(\psi + \frac{\pi}{3}\right)\right)^2\left(\left(\frac{\partial\chi}{\partial r}\right)^2 + \frac{1}{r^2}\left(\frac{\partial\chi}{\partial\vartheta} + 1\right)^2\right) \\ &+ \frac{8}{9r^2\sin^2\vartheta}\left(\cos^2(\chi+\vartheta)\sin^2\psi + \sin^2(\chi+\vartheta)\sin^2\left(\psi + \frac{\pi}{3}\right)\right).\end{aligned} \tag{12}$$

The anchoring conditions to be imposed on $\boldsymbol{Q}$ are such that it represents a uniaxial state with positive scalar order parameter and director along the normal to either the lateral boundary of the cylinder or the whole sphere.

3. Fine core structure

In a cylinder, point defects arise because the director field has the same energy in either *escaped* radial solutions found in [20] (see also [21, 22]). In the parametrization employed here, they are described by setting

$$\psi \equiv 0 \quad \text{and} \quad \kappa = \pm\kappa_{ER} \qquad \text{with} \quad \kappa_{ER}(\rho) := \tfrac{1}{2}\pi - \arctan\rho.$$

Wherever two opposite escaped fields meet, a point defect on the axis joins them together, exhibiting the fine structure described in [15]. There the uniaxial ring is the locus $\rho = \rho_{\mathrm{u}}$ in the plane $z = 0$ where $\psi = \frac{\pi}{3}$, while $\kappa \equiv \frac{\pi}{2}$ for $0 \leqslant \rho < \rho_{\mathrm{u}}$, and $\kappa \equiv 0$ for $\rho_{\mathrm{u}} < \rho \leqslant 1$. This is the only jump in κ that causes neither a singularity in the free energy nor a discontinuity in $\boldsymbol{Q}$, because for $\psi = \frac{\pi}{3}$ the coefficient of $|\nabla\kappa|^2$ in (11) vanishes, and by (5) a change by $\frac{\pi}{2}$ in κ does not affect $\boldsymbol{Q}$. However, $\nabla\psi$ may fail to be continuous along the uniaxial ring. In [15] the excess free energy is indeed minimized within the class of fields $\{\kappa, \psi\}$ with precisely these admissible jumps on a ring where $\psi = \frac{\pi}{3}$, which is otherwise free to vary in the plane $z = 0$. For h sufficiently large, the appropriate boundary conditions for $\{\kappa, \psi\}$ read as

$$\begin{aligned} &\{\kappa, \psi\}|_{\rho=0} = \left\{\tfrac{1}{2}\pi, 0\right\} \qquad \{\kappa, \psi\}|_{\rho=1} = \{0, 0\} \\ &\{\kappa, \psi\}|_{z=\pm\frac{h}{2}} = \{\kappa_{ER}, 0\}. \end{aligned} \tag{13}$$

It should be noted that by equation $(13)_1$ the singularity of $\sigma_e^{(\mathrm{c})}$ as $\rho \to 0$ can be made integrable in $(9)_1$.

Similarly, within a sphere the uniaxial ring lies in the plane $\vartheta = \frac{\pi}{2}$ at $r = r_{\mathrm{u}}$, where $\psi = \frac{\pi}{3}$, while $\chi \equiv -\frac{\pi}{2}$ for $0 \leqslant r < r_{\mathrm{u}}$ and $\chi \equiv 0$ for $r_{\mathrm{u}} < r \leqslant 1$. Along this ring the coefficient of $|\nabla(\chi + \vartheta)|^2$ in (12) vanishes, and by (5) $\boldsymbol{Q}$ is continuous. The boundary conditions for $\{\chi, \psi\}$ are

$$\begin{aligned} &\{\chi, \psi\}|_{\vartheta=0,\pi} = \{0, 0\} \qquad \{\chi, \psi\}|_{r=1} = \{0, 0\} \\ &\{\chi, \psi\}|_{r\to 0} = \{-\vartheta, 0\}. \end{aligned} \tag{14}$$

In the latter, which is required for the continuity of $\{\chi, \psi\}$ at the origin, the limit as $r \to 0$ is taken along a radius with constant ϑ. By $(14)_1$, the singularity of $\sigma_e^{(\mathrm{s})}$ along the polar axis can be made integrable in $(9)_2$.

The defect structure for both cylindrical and spherical confinements and different values of R are determined numerically by applying the relaxation method in [23] to the Euler–Lagrange

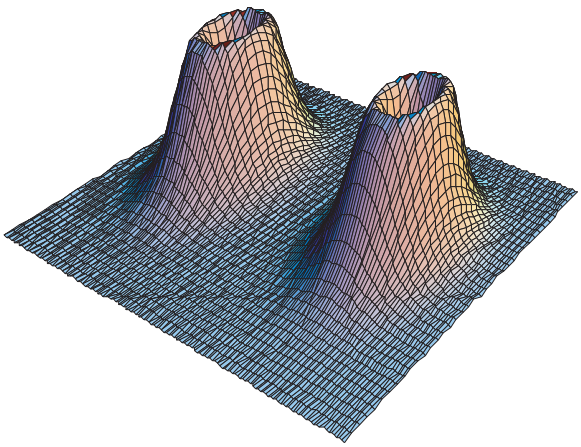

Figure 3. Logarithm plot of the degree of biaxiality β^2 on a plane through the symmetry axis of the core.

(This figure is in colour only in the electronic version, see `www.iop.org`)

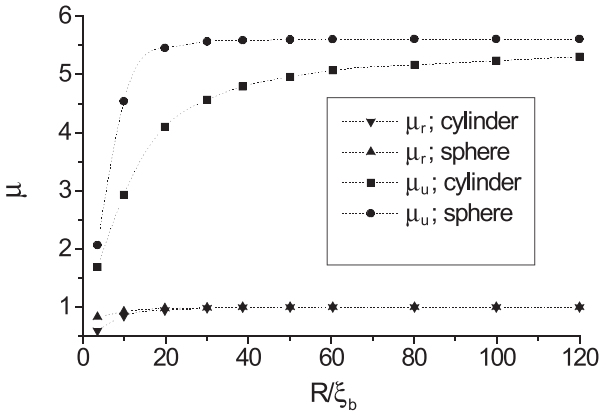

Figure 4. Effect of confinement on the uniaxial ring and the biaxial torus. Here $\mu_{\rm u} = \xi_{\rm u}/\xi_b$ and $\mu_{\rm r} = \xi_\perp/\xi_\parallel$, with $\xi_{\rm u}$ equal to either $\rho_{\rm u}$ or $r_{\rm u}$, and $2\xi_\perp$, $2\xi_\parallel$ the width and the height of the torus with a maximum degree of biaxiality.

equations for ΔF. Across the equilibrium uniaxial ring both $\Delta f^{(\rm c)}$ and $\Delta f^{(\rm s)}$ turn out to be continuous. There are two different length scales in our model, namely, the length R over which spatial distortions in κ or χ are typically exhibited for constant ψ, and the length ξ_b which defines the scale of variation for ψ. To calculate the defect structure in the limit $R \gg \xi_b$, we introduce the logarithm scales $u_\rho := \ln \rho$ and $u_r := \ln r$, both cut below an appropriate value u_c, for which we used $u_c = 10^{-3}$. For example, figure 3 illustrates the biaxial torus by showing the graph of β^2 as a function of (u_ρ, z) for the minimizer of $\Delta F^{(\rm c)}$.

The effect of the two different confinements on the biaxial structure of a point defect is shown in figure 4 by plotting the ratios between the lengths $\xi_{\rm u}$, $\xi_\parallel$ and $\xi_\perp$ against R/ξ_b. Here $\xi_{\rm u}$ denotes either $\rho_{\rm u}$ or $r_{\rm u}$, while $2\xi_\parallel$ and $2\xi_\perp$ are the height and the width of the torus cross section. For R large enough, precisely for $R > 20\xi_b$, the torus cross section is essentially circular in both confinements, whereas $r_{\rm u}$ is appreciably larger than $\rho_{\rm u}$. For even larger values of R ($R > 200\xi_b$), the whole core structure is almost the same for both confining geometries: in particular, for $R/\xi_b = 1000$, the two cores are indistinguishable within our degree of accuracy.

This fact clearly indicates that the defect core acquires a universal structure if the characteristic size of the confining cavity is large enough: in other words, the core structure does not depend on the far director field. Only the changes in the order parameter field ψ play a primary role in shaping the core of a hedgehog.

On the other hand, when R is decreased the torus cross section becomes increasingly prolate in the direction of the symmetry axis and all characteristic lengths decrease likewise. This effect is, however, far less pronounced in the spherical geometry than in the cylindrical one, as more room is left in the latter for the biaxial torus to remain anisotropic.

4. Stability of the biaxial core structure

So far we have examined the biaxial core structure around the uniaxial ring without questioning its stability versus the uniaxial hedgehog, which appears as its natural competitor. Here we show that deep in the nematic phase the biaxial core structure is indeed stable relative to the uniaxial one. More detailed stability analyses, where two elastic constants enter (4) instead of a single one, can be found in [8–10].

Consider a point defect at the centre of a sphere of radius R. In the uniaxial hedgehog around it, the scalar order parameter s defined in (2) fails to be constant: it vanishes at the centre of the sphere. Accordingly, here Lyuksyutov's constraint is no longer taken as valid. In addition to R, the relevant characteristic size of this structure is the nematic uniaxial correlation length ξ, which varies with the temperature T. In the appendix to [15] we arrived at the following expression for ξ:

$$\xi(\tau) = \xi_n \frac{\sqrt{2}}{\sqrt{-4\tau + \frac{9}{2} + \frac{3}{2}\sqrt{9-8\tau}}} \tag{15}$$

where

$$\tau := \frac{T - T_*}{T_{IN} - T_*}$$

is the *reduced temperature*. Here T_{IN} and T_* are the bulk isotropic–nematic transition temperature and the nematic supercooling temperature, respectively. Clearly, $\xi_n = \xi(1)$ is the nematic correlation length at the isotropic–nematic transition.

In terms of the reduced temperature the equilibrium value of the uniaxial order parameter $s_{\rm eq}$ reads as

$$s_{\rm eq}(\tau) = s_0 \frac{3 + \sqrt{9-8\tau}}{4} =: s_0 q$$

where $s_0 := \frac{B}{4C}$ is the value of $s_{\rm eq}$ at the isotropic nematic transition. Similarly, the biaxial correlation length ξ_b is a function of τ:

$$\xi_b(\tau) = \frac{\xi_n}{3\sqrt{q}}.$$

It should be noted that ξ is more influenced by the temperature than ξ_b: the ratio $\mu := \frac{\xi_b}{\xi}$ is a monotonically decreasing function of τ.

We have shown in [15] that for a line defect the biaxial structure is favoured energetically over the uniaxial structure whenever $\mu > 1$. Below we perform a similar comparison for the core structure of a point defect in spherical symmetry. The corresponding dimensionless excess free energy density is now expressed in terms of the scaled uniaxial order parameter $u := \frac{s}{s_{\rm eq}(\tau)}$ as

$$\Delta f^{(\rm u)} = \frac{1}{\xi_n^2}\sigma_b^{(\rm u)} + \sigma_e^{(\rm u)}$$

where

$$\sigma_e^{(\rm u)} = \frac{4u^2}{r^2} + \frac{2}{3}\left(\frac{\partial u}{\partial r}\right)^2 \tag{16}$$

$$\sigma_b^{(\rm u)} = \tfrac{2}{3}\left(u^2\left(\tau - 2uq + u^2q^2\right) - \left(\tau - 2q + q^2\right)\right). \tag{17}$$

Here the superscript (u) refers to the uniaxial core structure in the sphere. Accordingly, the excess free energy stored in the whole sphere is denoted by $\Delta F^{(\rm u)}$.

In figure 5 the ratio $\eta := \frac{\Delta F^{(\rm u)}}{\Delta F^{(\rm s)}}$ between the excess free energies for the uniaxial and biaxial core structures is plotted as a function of μ for three different radia. It turns out that $\eta > 1$ over the whole regime studied here, indicating the stability of the biaxial core structure versus the uniaxial one.

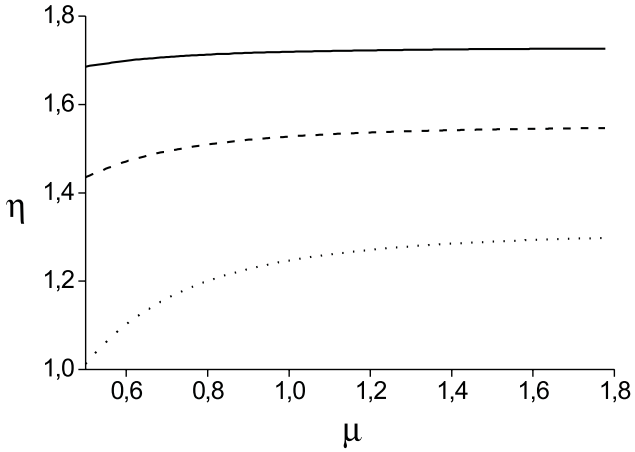

Figure 5. The ratio $\eta := \frac{\Delta F^{(\mathrm{u})}}{\Delta F^{(\mathrm{s})}}$ as a function of $\mu := \frac{\xi_b}{\xi}$ computed for $\frac{R}{\xi_b} = 10$ (dotted curve), $\frac{R}{\xi_b} = 100$ (broken curve) and $\frac{R}{\xi_b} = 1000$ (full curve).

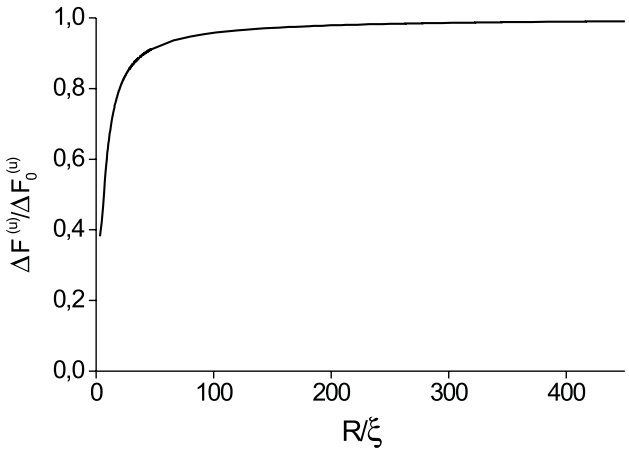

Figure 6. The ratio $\frac{\Delta F^{(\mathrm{u})}}{\Delta F_0^{(\mathrm{u})}}$ as a function of $\frac{R}{\xi}$: it is close to 1 for $\frac{R}{\xi} > 100$.

To compute the total free energy $\Delta F_0^{(\mathrm{u})}$ stored in the sphere when the uniaxial order parameter s equals its equilibrium value s_{eq} everywhere, it suffices to set $u \equiv 1$ in both equations (16) and (17), thus obtaining[5] $\Delta F_0^{(\mathrm{u})} = 16\pi$. Figure 6 illustrates the graph of the ratio $\frac{\Delta F^{(\mathrm{u})}}{\Delta F_0^{(\mathrm{u})}}$ as a function of $\frac{R}{\xi}$: the approximation of $\Delta F^{(\mathrm{u})}$ with $\Delta F_0^{(\mathrm{u})}$ then turns out to be rather good for $R > 100\xi$.

5. Conclusion

We imagined a geometric confinement on the fine structure of a nematic hedgehog. We considered only the case where the local topological frustrations in the uniaxial description

[5] To recover the most familiar expression for this energy, that is, $4\pi K R$, the reader should heed that here Frank's constant K equals $4Ls_{\mathrm{eq}}^2$ and all free energies are expressed in units of RLs_{eq}^2.

are removed without melting the nematic order. Our study indicates that the defect structure is universal if the characteristic confinement length (or separation between interacting defects in the bulk) is large enough relative to the typical biaxial correlation length. Thus the eigenvalues of $\boldsymbol{Q}$ play a primary role compared with its eigenvectors in shaping the defect core. In the opposite limit, the confining geometry is reflected on the core symmetry.

Acknowledgments

This research was supported by a bilateral cooperation between Italy and Slovenia. We thank S Žumer for an illuminating discussion on the universal core structure of a hedgehog.

References

[1] Mermin N D 1976 *Rev. Mod. Phys.* **51** 591
[2] Kleman M 1983 *Points, Lines and Walls* (Chichester: Wiley)
[3] Trebin H R 1998 *Liq. Cryst.* **24** 127 and references therein
[4] Kurik M V and Lavrentovich O D 1988 *Sov. Phys.–Usp.* **31** 196 (1988 *Usp. Fiz. Nauk* **154** 381) and references therein
[5] de Gennes P G and Prost J 1993 *The Physics of Liquid Crystals* (Oxford: Oxford University Press)
[6] Schopol N and Sluckin T J 1988 *J. Physique* **49** 1097
[7] Kralj S, Žumer S and Allender D W 1991 *Phys. Rev.* A **43** 2943
[8] Rosso R and Virga E G 1996 *J. Phys. A: Math. Gen.* **29** 4247
[9] Gartland E C and Mkaddem S 1999 *Phys. Rev.* E **59** 563
[10] Mkaddem S and Gartland E C 2000 *Phys. Rev.* E **62** 6694
[11] Schopol N and Sluckin T J 1987 *Phys. Rev. Lett.* **59** 2582
[12] Penzenstadler E and Trebin H R 1989 *J. Physique* **50** 1025
[13] Terentjev M 1995 *Phys. Rev.* E **51** 1330
[14] Lavrentovich O D, Ishikawa T and Terentjev E M 1997 *Mol. Cryst. Liq. Cryst.* **299** 301
[15] Kralj S, Virga E G and Žumer S 1999 *Phys. Rev.* E **60** 1858
[16] Biscari P and Virga E G 1997 *Int. J. Nonlin. Mech.* **32** 337
[17] Kaiser P, Wiese W and Hess S 1992 *J. Non-Equilib. Thermodyn.* **17** 153
[18] Monselesen D and Trebin H R 1989 *Phys. Status Solidi* **155** 349
[19] Lyuksyutov I F 1987 *Sov. Phys.–JETP* **48** 178
[20] Cladis P E and Kléman M 1972 *J. Physique* **33** 591
[21] Williams C, Pieranski P and Cladis P E 1972 *Phys. Rev. Lett.* **29** 90
[22] Meyer R B 1973 *Phil. Mag.* **77** 405
[23] Vesely F J 1994 *Computational Physics* (New York: Plenum)